



Universität Hamburg



German-Armenian Joint Practical Course on Accelerator Physics

Control and Operation of Femtosecond Lasers for Driving The Linear Accelerator

Supervisor: Dr. Arsham Yeremyan



Federal Foreign Office

*Supported by the German Federal Foreign Office
under Kapitel 0504, Titel 68713*

YEREVAN, ARMENIA
2019

Table of Contents

Summary of the practical work	2
Lab Safety Instructions.....	4
Introduction	5
1. High-energy, ultrashort-pulse lasers.....	8
1.1 MOPA architecture	9
1.2 AREAL laser system	12
2. Ultrashort-pulse lasers for bright electron beam sources.....	13
2.1 Photoinjector basics	14
2.2 AREAL schematic	15
3. Measurement of main laser parameters	16
3.1 Power/energy and repetition rate measurements.....	17
3.2 Beam profile measurement	19
4. Measurement of ultrashort laser pulse duration.....	21
4.1 The method of autocorrelation interferometry: theory and schematic description	21
Task 1. Measurement of duration of ultrashort pulses at different degree of compression.....	24
Instructions.....	24
Task 2. Laser pulse duration effect on energy spread of the accelerated electron bunches.....	28
Further Reading	28
APPENDIX A: Relationship among energy parameters.....	29
APPENDIX B: Report Table 1	30
Signature Sheet	31

Summary of the practical work

In this practical work, students perform measurements of ultrashort-laser pulses by using the output of the AREAL laser system, which provides pulses with variable parameters like energy/ power, repetition rate, and pulse duration.

In the preparatory PART 1 of the lab work, the students are given an overview of the laser system and some background on principle of operation and main characteristics of femtosecond lasers. An introduction to the basics of the laser-driven electron sources is given as a feature application of ultrashort-pulse lasers, details and schematics for AREAL facility are described. Students learn how to operate the laser system and configure the laser parameters using the driver software. With assistance and under supervision of the tutor, students measure the power, repetition rate, and beam profile on different nodes of laser output to get knowledge of the characteristics and performance of the system, as well as to acquire basic skills in optics alignment and measurements that are necessary for carrying out the next (*experimental*) part of the lab work.

The experimental PART 2 of the work consists of two tasks. Task1 is devoted to studying the autocorrelation method of measuring the time duration of ultrashort laser pulses. The students learn the basic theory behind the method in parallel with practical implementation and operation of the Autocorrelator setup. The aim of Task 1 is to derive the duration of ultrashort laser pulses from measurement of the second harmonic signal as a function of optical delay distance between two identical pulses. The aim of Task2 is to apply the acquired skills to operate the laser and previously obtained measurement results in an experiment on AREAL facility. In particular, the beam energy spread will be studied by varying the laser pulse duration. This task is performed jointly and in collaboration with the group of students involved in the corresponding Experimental Task of the Joint Course (“Electron Beam Parameter Measurements”).

Upon completion of this lab work, students are expected to obtain basic knowledge and hands-on experience in operation and characterization of femtosecond lasers. In the course of implementation of experimental tasks students will study and use direct and indirect methods of measurement of power, spatial, and temporal characteristics of femtosecond lasers. Correspondingly, they will gather work experience in an

optical laboratory and will acquire practical skills in using a number of optical and optoelectronic devices and related software. The experimental work is related to collection, analysis and interpretation of measurement results, and is therefore supposed to contribute also to students' report writing and presentation skills.

Lab Safety Instructions

Before starting the lab work, students pass an assessment check of the following “Lab Safety Instructions” and sign in a form stating the awareness of hazards and risks related with operation of the laser system.

The lab work will be performed using the output of “*s-pulse*” regenerative amplifier which is a IV class laser equipment and is hazardous for eye and skin.

Moreover, the output radiation beams in the lab are invisible to unequipped eye. Therefore, it is **mandatory to strictly follow** the safety instructions below:

- Pay attention to corresponding warning signs in the controlled area:



- Remove any items with reflecting surfaces from cloths and hands (such as watches, jewelry, etc.) before starting the work;
- Do not place items which are not a part of the measurement equipment on the laser beam path;
- The setup and/or removal of an optical element required for the measurement must be performed only after covering the laser beam path with a non-transparent shield or closing the laser shutter;
- Keep your eyes above the laser beam level (about 1 m above the floor) when the laser is turned on;
- Protective eyeglasses must be used when required;
- Do not block the laser beam by hand
- Electrical safety rules must be followed

Attention

The laser system is pre-aligned and ready for this practical course; and **there will be no major** routing and/or alignment procedures required for completion of the experimental tasks. Alignment procedures for teaching and/or demonstrations purposes **must be performed only** under the supervision of the tutor or trained personnel.

In addition, the optical laboratories require a clean environment in order to avoid deposition of dust on- and damage the optics. The laser laboratory is equipped with a conditioner with dust collecting filters. Nevertheless, the students are asked to wear the clean jacks and replacement shoes or polyethylene covers available at the entrance of the Laser room.

Introduction

Ultrashort laser pulses are the pulses of coherent electromagnetic radiation with time duration of the order of a picosecond ($1\text{ps}=10^{-12}\text{ s}$) or less. An exciting kind of lasers in this category, femtosecond lasers, are characterized with pulse duration of tens to hundreds femtoseconds ($1\text{fs}=10^{-15}\text{ s}$).

While the methods of generation of such short pulses were available long time ago, the widespread use of these lasers started only in recent decades, mainly, due to the development of the so called chirped-pulse amplification technique. The latter enabled the efficient amplification of ultrashort pulses to extremely high energies with compact laser systems. Consequently, femtosecond lasers have started to evolve from rather complicated instruments to applied laser tools in science, medicine and industry where they are used, for example, as optical probe for time-resolved studies, for analysis of biological material or the micro structuring of advanced material components. As a recognition of the role of the chirped-pulse amplification technique in such a progress its inventors, Gérard Mourou and Donna Strickland were awarded the Nobel Prize in Physics in 2018.

One particular area where application of ultrashort-pulse lasers lead to new developments and significant progress is the field of particle acceleration. An impressive example is application in an RF-driven photogun used as an electron source in linear accelerators (such as the AREAL Linac at CANDLER). Here, small-emittance, short electron bunches are produced by illuminating a photocathode with a laser and accelerating the photo-emitted electrons in high-gradient, radio-frequency (RF) fields up to relativistic energies. Using the ultrashort pulses for electron injection adds a new dimension in controlling the characteristics of the electron bunches which paves the way for development of new concepts in electron acceleration and unique applications in many fields such as time-resolved experiments, materials characterization, new coherent radiation sources, etc.

The detailed description of femtosecond laser technology and its applications is out of the scope of this course and students are referred to books and reviews on the subject [1-2, 5]. It is worth mentioning here, nevertheless, the two characteristics of ultrashort-pulse lasers from which the most of their unique applications are derived. Firstly, extremely short duration of pulses can be used to induce and measure ultrafast phenomena with temporal resolution of femtoseconds while minimizing heat

transfer to the target. Secondly, extremely high peak intensity of radiation can be achieved with such short pulses which lead to nonlinear and principally new regimes of light-matter interactions. Huge electric fields associated to the pulses can surpass, e.g. the electron binding energies of the atoms, resulting in large ionizations.

The benefits coming from ultrashort-pulse lasers are thus related with effects and processes that depend critically on different laser parameters. Therefore, the output characteristics of the laser beam, as well as stability and other performance figures need to be regularly measured, controlled and/or monitored for a process control and for reproducible experiments.

In this practical work, students learn to operate and control a femtosecond laser system and perform measurements of ultrashort-pulse lasers by using the output of the AREAL laser system. The Part 1 of the work is preparatory intended to give the students basic knowledge and skills required for operation and characterization of the laser system and for performing the experimental tasks. In Part 2, two experimental tasks will be carried out, in which students: 1) measure the duration of ultrashort laser pulses using the Autocorrelation method; and 2) study the effect of laser pulse duration on electron beam properties by applying the acquired skills to operate the laser and knowledge gained in a real experiment on AREAL facility.

The description of the lab work is organized as follows. Chapter 1 gives an overview on basic configuration and principles of high-energy femtosecond lasers of a specific class including the AREAL laser system. In Chapter 2, advantages of such lasers are discussed when specifically applied for bright electron sources in linear accelerators. Principle of operation of a typical photoinjector is described schematically and specified for the AREAL linac. Chapter 3 provides a background information about the measurement techniques and specifics of equipment used in this work for characterization and control of main laser parameters. Theory and description of Experimental Tasks are presented in chapter 4.

Given the space limitation a comprehensive coverage on femtosecond laser technology and characterization techniques cannot be given here. Therefore, the basic concepts and techniques used for generation, amplification, and characterization of ultrashort pulses are discussed in PART 1 in amount and depth just enough for understanding the role and function of the key laser components, beam delivery schematics, as well as for learning the operation and control of the

AREAL laser during an experiment. On the other hand, sections of PART 1 often contain details and explanations which are not necessary for understanding or completion of the experimental tasks. Such a supplement is intended to be used as a link for students who may want to further study a topic of interest using the recommended external resources while keeping up with the course description.

PART 1

1. High-energy, ultrashort-pulse lasers

The laser pulses with duration of less than ~ 10 ps, called ultrashort pulses, are generated using the **mode-locking technique** [1,2]. Using the variations of this technique—active, passive, or hybrid—it is possible to generate trains of pulses with duration as short as several femtoseconds ($1 \text{ fs} = 10^{-15} \text{ s}$). Despite the high peak powers available with such short pulses their application was limited since the energy-per-pulse (see **Appendix A** for definition of these quantities) is only on the order of nanojoules and there were no efficient ways to boost it until the mid-1980s. Things have changed, mainly, due to the development of the so called **chirped-pulse amplification (CPA)** technique. The latter enabled the efficient amplification of ultrashort pulses to extremely high energies with compact laser systems.

Currently, there are many different types of femtosecond lasers using the CPA approach.

The following sections present an introduction to a particular type—**passively mode-locked, diode-pumped solid-state lasers**—which are the most widely used systems providing high-quality, high-energy, ultrashort pulses for various applications. The laser system which drives the AREAL Linac is a representative of this class of femtosecond lasers and its features will be specifically described.

Even with such restriction, a comprehensive coverage cannot be given in this practical work. Therefore, the basic concepts and techniques used for generation, amplification, and manipulation of characteristics of ultrashort pulses are discussed here in volume and depth just enough for understanding the role and function of the key laser components, beam delivery schematics, as well as for learning the operation and control of the AREAL laser during the experiments.

In order to complete this practical lab work, it is assumed that students have a basic knowledge of laser theory and technology. For more details on the underlying physics and principle of operation of key components of the system, students are specifically referred to teaching materials and handbooks on theory and technology of femtosecond lasers, including those recommended in this course [1-3].

1.1 MOPA architecture

Most of the high-power laser systems are based on the so-called **MOPA**¹ (**Master Oscillator Power Amplifier**) configuration, in which the energy of a weak light pulse generated from a laser oscillator is subsequently increased in an amplifier. Such an architecture is advantageous in many respects over a laser which directly produces the required high energy. This gives more flexibility since it allows decoupling of various performance characteristics from the high-power generation. For example, additional optical components such as wavelength tuning elements can be placed in the oscillator to avoid the damage due to high intensities. On the other hand, the characteristics such as beam quality and pulse duration may be easier to control at high-power levels.

The MOPA configuration is particularly suitable for implementation of CPA scheme which is illustrated on **Figure 1.1**. The scheme works as follows.

- (1) Ultrashort light pulses are generated at low pulse energy using an ultrashort-pulse mode-locked **laser oscillator**. The oscillator typically generates pulses at a high repetition rate (10s to 100s of MHz) with pulse energies in the range of nano-Joules, and with pulse durations in the range of 10^{-12} – 10^{-14} s.
- (2) These femtosecond pulses are then chirped using a dispersive delay line consisting of either an optical fiber or a diffraction-grating arrangement. The pulse is typically **stretched** to ~100 ps, decreasing its peak power by orders of magnitude.
- (3) One or more stages of laser amplification are used to increase the energy of the pulse by six to nine orders of magnitude to efficiently extract energy from the laser amplifiers. This amplification typically requires a total of between 4 and 50 passes through an amplification medium, with a gain of between 2 and 100 per pass.
- (4) After optical amplification, when the pulse is very energetic, a second grating pair is then used to **recompress** the pulse back to ultrashort duration. To achieve this recompression back to near the original input pulse duration, proper optical design of the amplifier system is very important.

¹ The term “Master Oscillator” here refers to a femtosecond laser source and should not be confused with that used throughout this practical course for the electronic RF generator driving the Linac.

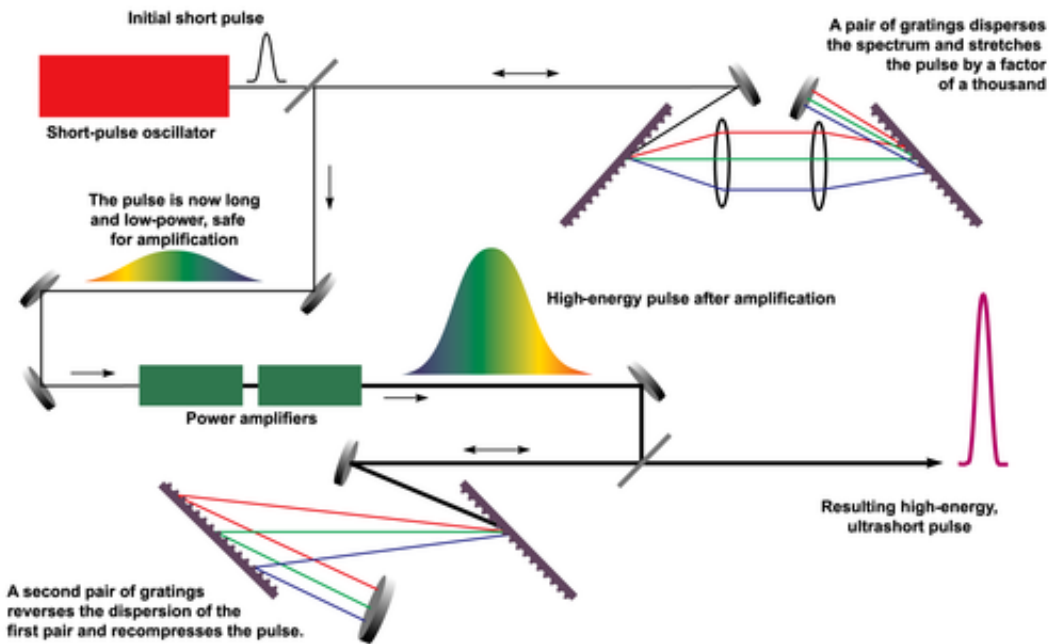


Figure 1.1. Schematic of MOPA-configuration with chirped-pulse amplification. Drawing from https://en.wikipedia.org/wiki/Chirped_pulse_amplification .

While the schematic presented in **Figure 1.1** is quite general and describes the most of the solid-state laser systems, the implementation of different parts varies depending on the desired laser characteristics and application requirements. The parts **(1)** to **(4)** of the schematic are further discussed below.

(1) Laser oscillators. Due to a range of specific properties Titanium-doped sapphire ($\text{Ti}^{3+}:\text{Al}_2\text{O}_3$ or Ti:Sapphire) is the most widely used crystal for femtosecond solid-state lasers. In particular, the very large gain bandwidth of the Ti^{3+} ion allows the generation of very short pulses while providing also a wide wavelength tunability. Nevertheless, other gain media are also widely used which may have specific advantages and provide superior performance for particular applications. **Table 1.1** represents a selected list of materials used as gain media for mode-locked laser systems.

Most common solid-state materials used as gain media are those with a long (compared to typical cavity round-trip times) fluorescence (upper-state) lifetime.

(2) Pulse stretching takes the advantage of the fact that femtosecond pulses have an intrinsically broad spectrum; pulse duration and its spectrum are related by:

$$\Delta\tau \Delta\nu > k,$$

where k is a constant depending on the pulse temporal shape. This allows to implement a spectral “chirp” using diffraction gratings.

Table 1.1. Selected list of solid-state laser systems and their operating parameters, Ref. [5].

Host	Dopant	Wavelength [μm]	Band Width [nm]	Gain Cross Section [$\times 10^{-20}$ cm ²]	Upper State Lifetime [μs]
YAG	Nd	1.064	0.6	33	230
YLF	Nd	1.047-1.0530	1.2	18	480
Vanadate	Nd	1.064	0.8	300	100
Phosphate Glass	Nd	1.0535-1.054	24.3	4.5	323
KGW	Yb	1.030	25	2.8	250
YAG	Yb	1.030	6.3	2.0	950
Phosphate Glass	Yb	1.06-1.12	62	0.049	1 300
Sapphire	Ti	0.790	230	41	3.2

In **Figure 1.1**, the pulse stretcher incorporates two diffraction gratings introducing path length dependence on the optical wavelength: optical path seen by a short-wavelength spectral component (“blue”-part) is longer than that seen by a long-wavelength spectral component (“red”-part). The “blue” part of the spectrum is therefore delayed in the pulse stretcher. As a result, the pulses are **spectrally chirped** on the output of the stretcher. It should be noted here, that “blue” and “red” both in the text and on the figure are used to denote “shorter” and “longer” wavelengths and should not be understood literally.

(3) Amplifier system can be a regenerative amplifier, a linear multi-pass amplifier, or a series of these.

In a regenerative amplifier, a Pockels-cell switching module traps a single pulse from the train of oscillator beam and injects it into the resonant cavity containing the excited gain medium. After several passes through the medium and the corresponding increase in energy, the pulse is ejected from the cavity typically by the same or another Pockels cell. The delay between the injection- and extraction-time determines the number of passes through the gain medium, as well as the highest repetition rate that the amplifier can support.

A multi-pass amplifier differs from the regenerative amplifier in that the gain medium is not a part of a resonant cavity. Therefore, the multiple passes through the gain medium required to boost the energy of the seed pulses are arranged via a geometrical path instead of the round-trips of the pulses in a regenerative amplifier implemented with opto-electric switches.

Each of these types of amplifiers has its advantages and limitations and the choice is dictated by the cost and a particular application. Multi-pass amplifiers have a lower

cost, whereas the regenerative amplifiers may provide superior performance characteristics.

(4) *The pulse compressor* is similar in principle with the pulse stretcher (Figure 1.1) except that it reverses the dispersion of the stretcher gratings and the "blue" part of the spectrum sees a shorter optical path than the "red" part. As a result, pulses are recompressed.

1.2 AREAL laser system

The AREAL laser, Figure 1.2, is a commercial system built in the MOPA configuration described above and is a passively mode-locked, solid-state laser with an amplifier providing ultrashort laser pulses with energies at mJ level. The system consists of the "t-pulse" oscillator, "s-pulse" regenerative amplifier including the *stretcher/compressor* modules, as well as the *4th-harmonic generation module (FHG)*, for non-linear optical conversion of the laser fundamental IR wavelength to UV for driving the Linac photocathode.

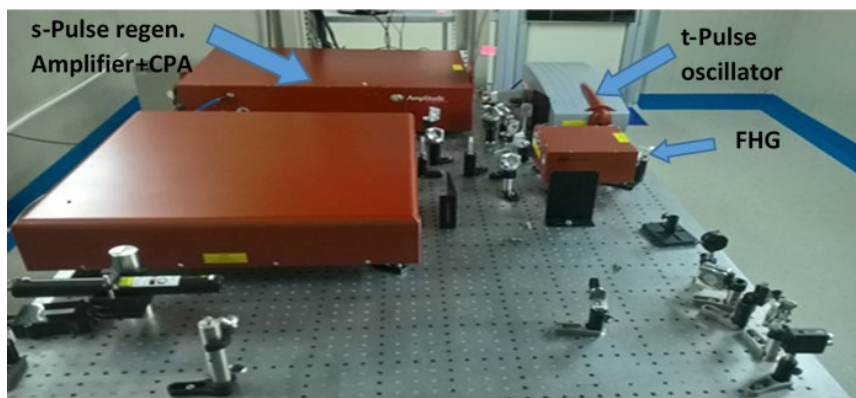


Figure 1.2. AREAL laser system consisting of "t-pulse" laser oscillator, "s-pulse" regenerative amplifier with stretcher/compressor modules, and the 4th Harmonic generation module, FHG. Supplier: **Amplitude Systemes** www.Amplitude-laser.com

The gain medium for both "t-pulse" oscillator and "s-pulse" amplifier is Ytterbium-doped potassium gadolinium tungstate crystal: $\text{Yb}^{3+}:\text{KGd}(\text{WO}_4)_2$ or $\text{Yb}:\text{KGW}$. The latter exhibits strong absorption band in the near infrared (typically 940-980 nm), which allows direct pumping with high-power diodes. The fluorescence spectral bandwidth of Yb is large enough (see Table 1.1) to sustain the amplification of ultrashort laser pulses.

The mode-locking for ultrashort pulse generation is implemented in "t-pulse" by **saturable absorber mirror (SAM)**, and the laser operates in the "Soliton" regime, in which the cavity parameters are adjusted to achieve a stable equilibrium between the

various dispersive and non-linear effects. In addition, the system is equipped with a ***synchronization unit*** which allows to fine-tune the repetition rate and preserve the synchronization of the laser with the RF Master Oscillator of Linac (see the following chapter). For this purpose, SAM is mounted on stepper-motor and piezo-driven stages to compensate for thermal instabilities and the fast changes in the cavity length.

The specifications of “*t-pulse*” and “*s-pulse*” lasers and the tuning range of their parameters are summarized in **Table 1.2**.

Table 1.2. “*t-pulse*” and “*s-pulse*” parameters.

	<i>t-pulse</i>	<i>s-pulse</i>	FHG
Wavelength	1030 nm	1030 nm	258 nm
Pulse width	230 fs	400 fs—8 ps	400 fs –8 ps
Rep. Rate	50 MHz	1Hz--100 kHz	1Hz—1 kHz
Energy/pulse	up to 20 nJ	up to 2 mJ	up to 425 uJ

Most of the laser parameters can be set via PC using a LABVIEW-written Software.

Detailed description and principle of operation of “*t-pulse*” laser oscillator and “*s-pulse*” regenerative amplifier, as well as hardware and software user manuals are available for reference during the lab work.

2. Ultrashort-pulse lasers for bright electron beam sources

Production of high-brightness electron beams is a key aspect of accelerator physics and technology since the success of many high-impact applications, such as linear colliders and free-electron lasers depends on the availability of such electron sources.

Due to the application in ***RF-photoinjector*** sources ultrashort-pulse lasers have had an especially high impact on the progress in this field. Invented practically in the same year with chirped-pulse amplification (in 1985), the RF-photoinjectors driven by ultrashort laser pulses have since become an essential instrument in accelerator physics and technology, enabling the production of intense, relativistic electron beams with ultra-fast time structures.

The comprehensive theory of photoinjectors involves a wide range of accelerator physics topics—from the material science of cathodes to the dynamics of electrons in magnetic and RF fields. Moreover, the strong effects the electrons have upon each

other in their mutually repulsive fields, i.e. space charge fields, have to be considered as well. Most of these topics are discussed in detail in [5].

2.1 Photoinjector basics

Emittance and **brightness** are important figures of merit largely used for electron beams¹. The emittance is a measure for the average spread of particle coordinates in position-momentum phase space (6D-phase space). The brightness depends on beam current and emittance and is used as a measure of electron volume density. It is usually defined² as the beam current divided by transverse normalized emittances in two directions. It is, therefore, natural to consider the combination of high peak current and low emittance (along with the small energy spread) as a means for production of high-brightness electron beams. Due to its principle of operation and availability of high-peak power driving lasers, RF-photoinjectors have proven to offer such a combination enabling production of quality electron bunches.

The principle of operation of a typical RF-photoinjector is illustrated in Figure 2.1. The photoinjector consists of an electron gun which is an RF-powered cavity with a photocathode placed on its entrance. The laser pulses give electrons in the photocathode enough energy to overcome the material's work function and escape into vacuum. The emitted electrons are rapidly accelerated in the cavity to relativistic energies using the RF-electric field.

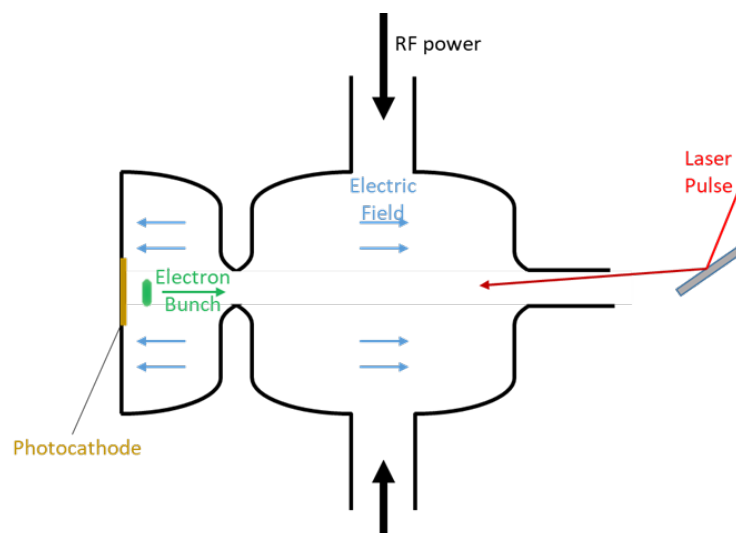


Figure 2.1. Principle of operation of a laser-driven RF-photogun.

¹ see ch.1 of Ref. [5] for further explanation of definitions.

² Different definitions of brightness are given in the literature depending on the subject field (see, for instance, Task description "Electron Beam parameter measurement" of this Joint Course). Terminology and definitions used here are those conventionally used in Photoinjector physics and technology.

Photoemission has several advantages over other methods commonly used for generation of high-current beams—field electron emission, thermionic and explosive emissions. Since the photo-effect described above is a non-inertial process it allows to control more precisely the longitudinal size of the beam. At the same time, the transverse size of the electron beam can be reduced by focusing the laser beam. Finally, the tunability and short pulse nature of the lasers together with the ability to synchronize them to sub-ps level with RF-fields make them ideal drivers for particle injectors to linear accelerators.

2.2 AREAL schematic

The description of the mechanism of photoemission and acceleration given in section 2.1 (Figure 2.1) is simplified and does not include all the aspects and parts which are nonetheless essential for successful generation of quality electron bunches.

Figure 2.2. and **Figure 2.3** illustrate the schematic layout of AREAL facility and the laser beam delivery scheme, respectively.

A discussion on physical bases and technical details related with different aspects of this general scheme will be given during the lab work. For more in-depth study of different aspects—such as photoemission, synchronization, or design considerations, students can consult the relevant topics of [5] and [6], and references therein.

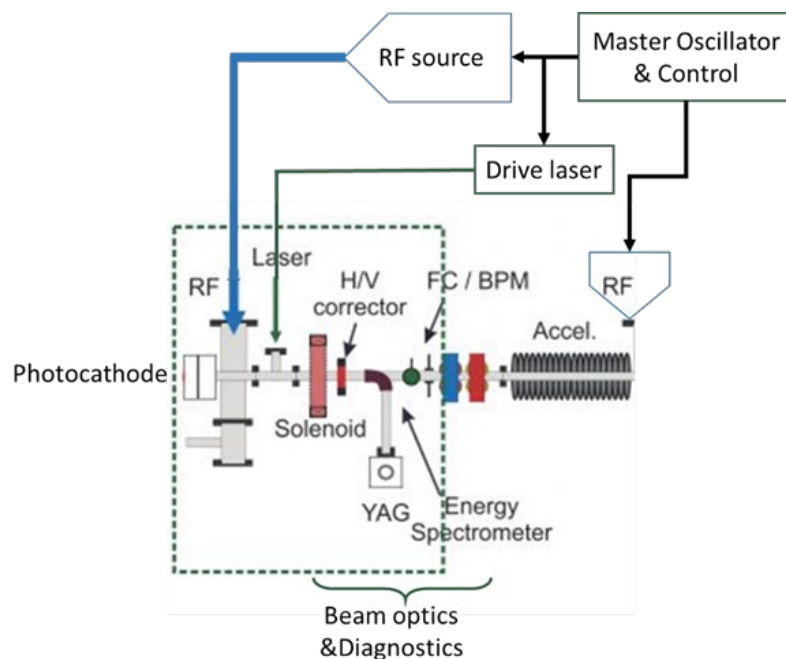


Figure 2.2. Schematic layout of AREAL facility.

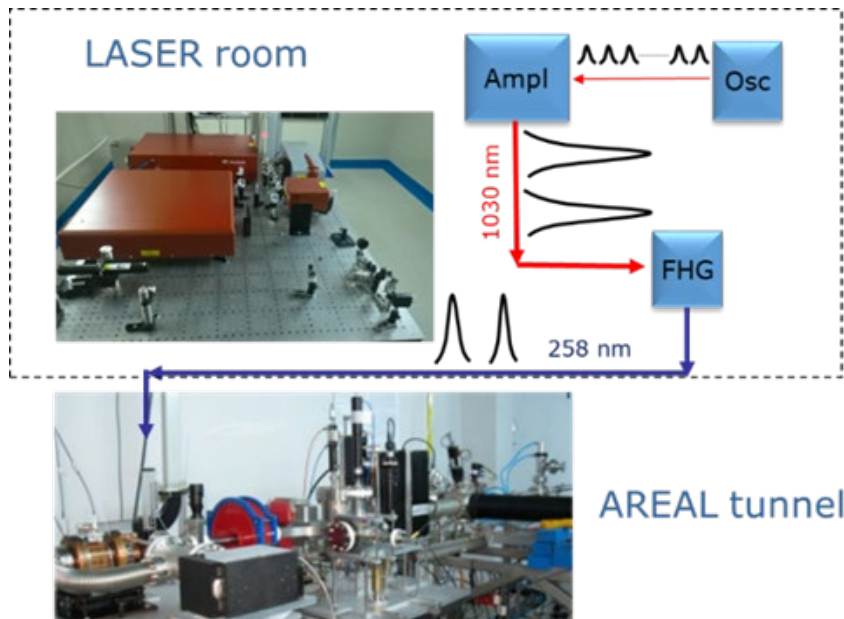


Figure 2.3. Laser beam routing to AREAL facility

3. Measurement of main laser parameters

A comprehensive analysis of a laser system involves measurements of a large set of parameters which define its overall performance and use for a specific task. Moreover, depending on the application, variation or tuning of certain laser parameters is often required for a process control or when selecting a desirable mode of operation. This is the case, namely, for a photoinjector since, as discussed above, the properties of output electron bunches largely depend on parameters of the driving laser. Therefore, the output power or energy, spatial and temporal characteristics of the laser beam, as well as its stability and other performance figures need to be regularly measured, controlled and/or monitored.

The following sections give a short description of the instruments and techniques that will be used in this part of lab work for measuring key laser parameters.

The basics on the principle of operation of an instrument, as well as the meaning and role of the measured quantities will be further discussed during the lab work. For more in-depth study of the related subjects, students are encouraged to explore the web resources using the key definitions and equipment information (vendor's name, model) presented here; knowledge bases, as well as the tutorials and manuals provided by most of the device vendors may serve as a good starting point for this purpose.

3.1 Power/energy and repetition rate measurements

An important parameter of a laser is its output power. Laser power measurement systems usually consist of two components. First is a sensor which is placed into the beam and converts the laser input to a proportional signal. The second instrument is the meter which interprets and measures the sensor signal and references it to a calibration chart to output the data. These data are then sent to a display unit or to a PC and are represented as a value or a graph in power units.

The most commonly used technologies for laser power sensing are pyroelectric sensors, thermopiles, and semiconductor photodiodes. Due to their working principles, the three detector types have different response characteristics such as wavelength response range, dynamic range, damage threshold, or response time¹. Selection of an instrument therefore depends on the characteristics of the source to be measured.

Furthermore, whereas the output power of a continuous wave (CW) laser is unambiguously defined and can be measured simply by using a system with suitable response characteristics, several other quantities come into play in the case of pulsed lasers. The choice of a measuring instrument in this case will depend, in particular, on whether the average power or the energy per pulse needs to be measured. Therefore, one often needs to know the relationships among some basic quantities when working with pulsed sources. Relationship between basic energy parameters is illustrated in **Appendix B**.

The three types of instruments discussed above are used for power measurements at different nodes of the AREAL laser system. Information on the model and vendor of instruments included in the captions of corresponding figures can serve as a reference for further details on principle of operation and specifications.

Pyroelectric detectors, **Figure 3.1a**, allow to measure pulse energy in repetitive pulse trains and is used to monitor the high-energy IR output of the “s-pulse”, as well as to measure the energy of the UV pulses supplied to the photocathode (cf. **Table 1.2**). Repetition rates up to 25 kHz can be registered for not very low energy-per-pulse, and the average power correspondingly represented.

¹ See also discussion on the response time in Section **4.1**.

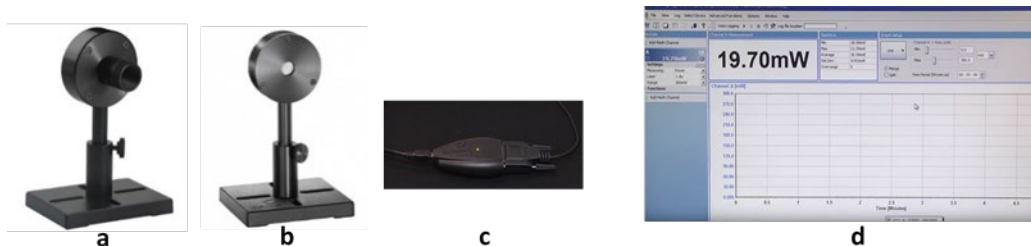


Figure 3.1. (a) pyroelectric sensor, **model PE10-C** (b) low-power thermal sensor, **model A10** (c) plug-and-play virtual meter and USB interface **Juno** for both (a) and (b); (d) a screenshot of the UI of the laser measuring software, **StarLab v.2.3**. Ophir Optronics **Ophir®**, www.ophiropt.com

Thermopiles or thermal sensors (**Figure 3.1b**) work over a broad range of wavelengths and input powers. Its primary use for the AREAL laser is to monitor the average power of the low-energy pulse, high-repetition rate beam of the “t-pulse” oscillator.

Semiconductor photodiodes offer the highest sensitivity and fastest response time among the considered detectors and enable one to register very low light intensity from high-repetition rate sources. Detectors of this type are permanently installed in several key nodes of the AREAL laser system—both internally and externally, and provide essential signals to controlling electronics of the laser or to the synchronization unit.

A *biased silicon photodiode*, in particular, is used for measuring the **repetition rate** of the “t-pulse” oscillator and for providing a pulse-train signal to the synchronization unit for tuning the laser cavity length via an electronic feedback control. This type of photodiodes usually has a BNC out for visualization of the signal on an oscilloscope (**Figure 3.2**).

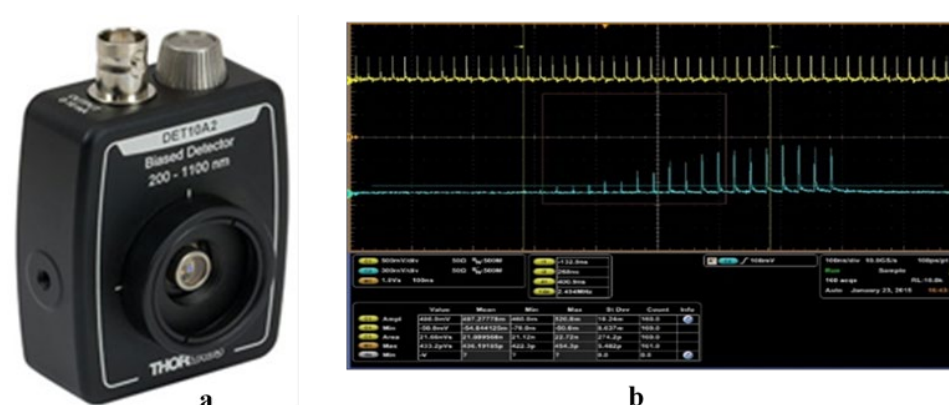


Figure 3.2. (a) biased Si-detector **model Det10A2**, Thorlabs www.thorlabs.com (b) scope acquisition of the signals from a detector measuring the “t-pulse” oscillator (yellow) and from an internal detector monitoring the pulse round trip in “s-pulse” resonator (cyan).

Another measuring system based on a *silicon photodetector* and a power meter (see **Figure 3.3**) is installed in the Autocorrelator setup and will be used during the Experimental Task of this lab work (Section 4.1).



Figure 3.3. (a) UV enhanced silicon photodiode of *model 918D-UV-OD3R* (b) Power meter of *model 1936-R*; Newport, MKS Instruments, www.newport.com .

3.2 Beam profile measurement

One of the important characteristics of lasers is the **spatial intensity profile** of the beam, i.e. the power density distribution in the plane perpendicular to the beam propagation direction. Analysis of the **beam profile** provides an information on the beam spatial characteristics such as size, position, shape, propagation, and mode structure. This information is key not only for maintaining the optimum laser system performance, but also for achieving the process-specific beam parameters in various applications.

In this sense, a photoinjector in electron accelerator is an illustrative case. For instance, the transverse profile of electron beams can be predicted and quantitatively related to the spatial characteristics of the laser beam since the shape of the laser beam is transferred almost undistorted on the photo-ejected electrons. Therefore, the emittance and other electron beam parameters can be improved by measuring and monitoring the laser parameters such as spot size, degree of uniformity, etc.

Beam-profile measurement (or beam profiling) techniques can be divided into two categories depending on the measurement principle: aperture-based and camera-based (or imaging) techniques.

The beam sampling in aperture-based techniques—such as knife-edges, slits and circular apertures is performed by scanning the aperture through the beam in the measurement plane and measuring the power behind the aperture. The beam profile is then the plot of the power vs. position.

The camera-based techniques have become popular and found the most widespread use with the availability of high-resolution cameras using two-dimensional CCD or CMOS sensor arrays. The intensity of the beam in this case is recorded pixel-by-pixel by individual sensors and the entire beam image is taken simultaneously. The latter is digitized and interfaced with a PC to perform 2D- or 3D-profile plots and full beam analysis using a dedicated software.

Due to the measurement principle, the camera-based technique is more suitable for pulsed laser characterization and will be used during this lab (**Figure 3.4**).

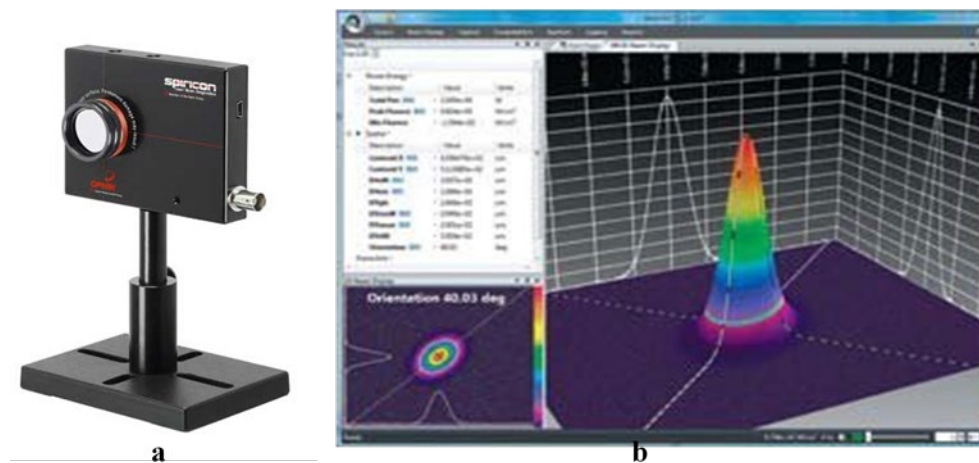


Figure 3.4. (a) Beam profiling camera *Spiricon model SP-620* (b) Beam profiling Software. Ophir Optonics *Ophir*®, www.ophiropt.com

PART 2

4. Measurement of ultrashort laser pulse duration

While the most of the femtosecond laser parameters such as power, wavelength, beam profile can be measured directly with sufficient accuracy using currently available devices and equipment, there are no direct methods of precise measurement of ultrashort pulse duration, or “pulse width”.

The traditional methods of optical pulse-width measurement, as discussed in *Section 3.1*, are generally based on using a photosensitive element and converting the electrical signals to a recordable form. The problem in the case of ultrashort pulses is that every photosensitive element has a limit of temporal resolution. For example, human eye and brain are able to process an optical signal in milliseconds. Using the semiconductor photodetectors, photomultipliers and similar devices allows to significantly increase the registration speed, but the latter is limited with charge relaxation processes which are of the order of 10s of picosecond.

Therefore, direct measurements of laser pulses with duration less than 20ps using photo detectors remain a challenge. The response time of high-speed photodiodes is currently limited to around 20 picoseconds; moreover, large bandwidth oscilloscopes (>60 GHz) required to accurately measure the output of these detectors are quite expensive.

Nevertheless, there are several indirect methods for measuring ultrashort pulses. Autocorrelation is the simplest and most affordable method for determining pulse width when phase information of the pulse is not required. For details on this and other methods (such as cross correlation, FROG, etc.) we refer to a book by R. Trebino [3,4], or by J.-C. Diels and W. Rudolph [1].

4.1 The method of autocorrelation interferometry: theory and schematic description

The autocorrelator setup is schematically illustrated in **Figure 4.1**. The principle of operation is based on recording the second order correlation function using a Michelson Interferometer.

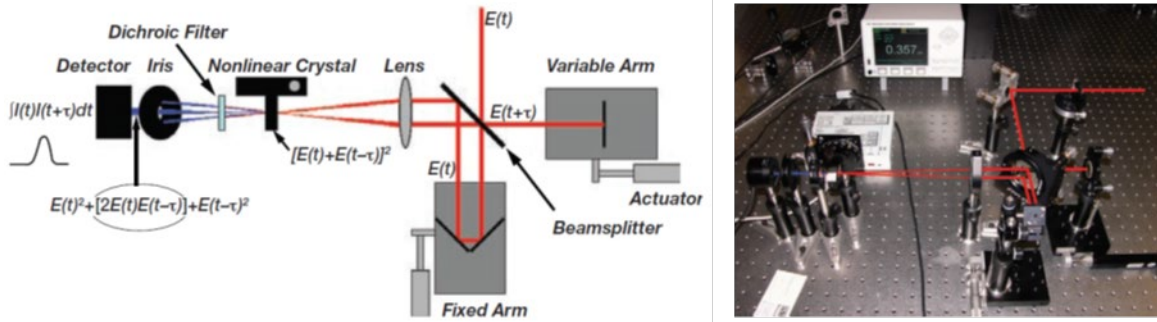


Figure 4.1 Schematic of the autocorrelator setup

An incoming pulse with electric field $E(t)$ is first split into two copies by means of a **Beamsplitter**. The two copies are sent to independent delay lines, one **Variable** and one **Fixed**, in order to generate a time delay between the two copies. The two replicas, $E(t)$ и $E(t + \tau)$, then pass through a **Lens** and recombine in a **Nonlinear Crystal**. Under proper phase matching conditions, a second harmonic signal (i.e. a signal at wavelength of half of the initial light) is generated in the crystal. The total intensity of the second harmonic signal $I_{SH}(t + \tau)$, is proportional to

$$I_{SH}(t + \tau) \sim [E(t) + E(t + \tau)]^2 \quad (4.1)$$

or

$$I_{SH}(t + \tau) \sim E^2(t) + [2E(t)E(t + \tau)] + E^2(t + \tau) \quad (4.2)$$

The component of the second harmonic, $[2E(t)E(t + \tau)]$, will only be present when the two pulses are overlapping in time. In the case that the two beams (two pulses) enter the crystal in a non-collinear geometry as shown in Figure 4.1, and when the phase matching conditions are satisfied only for the two-beam contribution, we obtain from equation (4.2),

$$I_{SH}(t + \tau) \sim [2E(t)E(t + \tau)] \quad (4.3)$$

The **Dichroic Filter** placed immediately after the **Nonlinear Crystal** suppresses the beam at fundamental wavelength (in our case, 1030 nm infrared) and transmits the second harmonic beam (in our case, 515 nm green). The **Iris** positioned after the crystal blocks the two initial replica beams, and the middle second harmonic beam is sent to a **Detector**.

Besides converting the second harmonic to an electrical signal, the **Detector** serves to square the incident field as well as integrate over the duration of the femtosecond pulse, t . The amplitude of the photo detector signal, $I_{AC}(t)$, is then proportional to,

$$I_{AC}(\tau) \sim \int [2E(t)E(t + \tau)]^2 dt \quad (4.4)$$

or, by relating the square of the electric field to intensity

$$I_{AC}(\tau) \sim \int [I(t)I(t + \tau)] dt \quad (4.5)$$

Equation (4.5) is formally a correlation integral and illustrates that the autocorrelation does not actually measure the pulse width directly, but a correlation function of the two copies. If the two replicas are indeed identical, then Eq. (5) can be solved analytically and the pulse width can be determined by dividing the autocorrelation signal width by a constant factor that depends on the profile of the pulse. The parameters for some common pulse profiles are listed in **Table 4.1**.

Table 4.1. Pulse profiles with corresponding autocorrelation functions*

	Pulse profile, $I(t) \sim$	Autocorrelation, $I_{AC}(\tau) \sim$	$\frac{\tau_{AC}}{\tau_p}$
Gaussian	$e^{-4Ln2 * (\frac{t}{\tau_p})^2}$	$e^{-4Ln2 * (\frac{\tau}{\tau_{AC}})^2}$	1.41
sech ²	$sech^2 [2Ln(1 + \sqrt{2}) \frac{t}{\tau_p}]$	---	---
Lorentzian	$[1 + \frac{4}{1 + \sqrt{2}} (\frac{t}{\tau_p})^2]^{-2}$	---	---

* Derivation of the omitted values of some cells is left as a task for assessment.

In summary, based on the described method, the following simple procedure is applied for determining the duration (width) of short laser pulses: a) the second harmonic signal is registered as a function of the of optical delay distance between two pulses; b) the registered data can be represented in time domain by converting the delay distance to time coordinates; c) using the computer, the functions are determined (Gaussian, Lorentzian, etc.) which give the best fit to the registered data; d) the pulse duration is finally determined by applying the factors corresponding to autocorrelation function (see **Table 4.1**).

Experimental Tasks

Task 1. Measurement of duration of ultrashort pulses at different degree of compression

The aim of this experimental Task is to study the method of autocorrelation for measurement of the duration of ultrashort laser pulses. Using the LABVIEW-based software, the best fit to measured autocorrelation function is found and pulse width is determined assuming different profiles for the laser pulse (Gaussian, sech^2 , etc.). By varying the position of the pulse compressor unit inside the “s-pulse” amplifier, the dependences of the pulse width on the position are derived at different repetition rates of the laser to provide an experimental parameter range for AREAL linac experiments. Experimental results are summarized, discussed and reported in the form of graphics and data files.

Instructions

Students are introduced to the parameters and specifications of optical, opto-mechanical, and measurement units of the uFAB Autocorrelator (**Figure 4.1**): optics damage threshold energies, control/measurement ranges, etc. LABVIEW-based software “Autocorrelator 3.4.4” for control and data acquisition/analysis software is described; the software user manual is provided for reference; General instructions and tips are given on safe operation of equipment and opto-mechanics.

A. Start-up condition

- “s-pulse” laser is turned on, the beam routed to the uFab laboratory, driver software is launched. Make sure that **Shutter** is in **CLOSE** position on the **Laser** menu of the “s-pulse” driver software (**Figure T1a**);

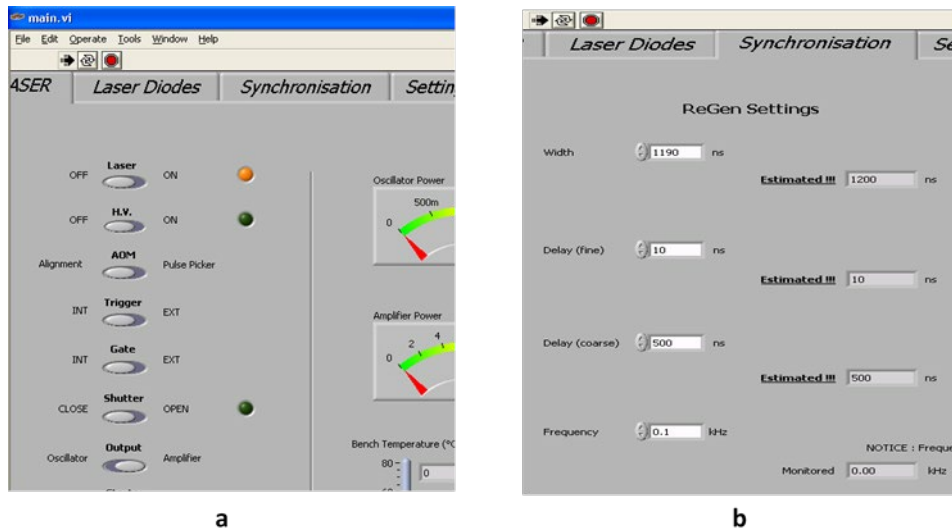


Figure T1. Screenshots of the “s-pulse” driver software UI

- The basic optical scheme of the autocorrelator is set up, controlling equipment is turned on, and control-measurement software are launched.
- Set the repetition rate, R , to a value in the range 20--1000 Hz (0.02--1kHz) in **Frequency** field on **Synchronization** menu of the “s-pulse” driver software **Figure T1b**;
- Position the “s-pulse” compression unit to a pre-set value using the user interface of the dedicated software, **Figure T2**.

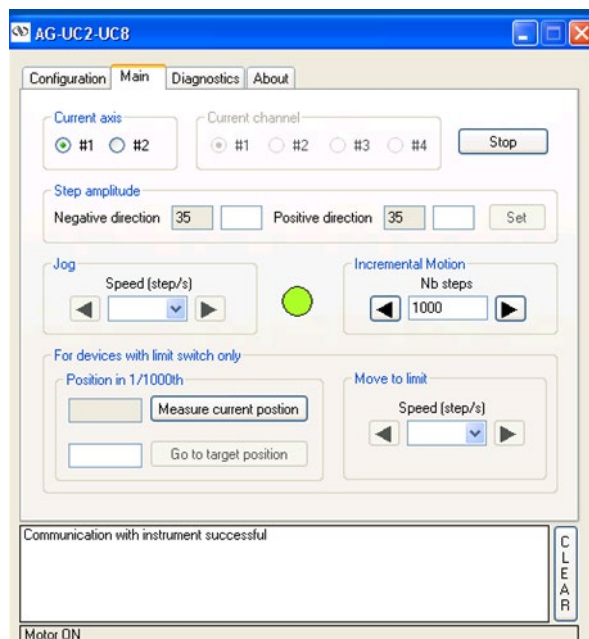


Figure T2 Interface of the pulse compressor driver

- Make sure that the beam to the Autocorrelator is blocked with a shield positioned after an entrance mirror;
- Open the **Shutter** from the **Laser** menu of the “*s-pulse*” driver software;
- Measure the pulse energy of the main beam, E_{tot} , by positioning the Pyro detector before the half-waveplate of the beam attenuator;
- Position the Pyro detector after the beam attenuator and note the energy of the pulses, E_p , passed directly through the beam attenuator;
- By slowly rotating the half-waveplate of the beam attenuator, reduce the energy of the beam to Autocorrelator, E_s , so that it's just sufficient to visualize the beam path in Autocorrelator using an IR viewing card or a luminescent paper;
- **TIP:** If E_s is beyond the sensitivity of Pyro detector, its value can be deduced by measuring E_{tot} and E_p and assuming constant insertion losses for the beam attenuator;
- Unblock the beam to the Autocorrelator;
- Using an IR viewing card or the IR viewing camera, check the paths of the replica beams in the Autocorrelator from the entry mirror down to the **Photodetector**, according to **Figure 4.1**;
- Make beam alignments for Autocorrelator setup if necessary, by tip/tilt adjustment of the entry mirrors;
- Block the beam to Autocorrelator and zero the power meter.
- Unblock the beam and optimize the power of the second harmonic signal using the micrometer on **Fixed delay line** and the tip/tilt adjustment on the mirror mount of **Variable delay line**, **Figure 4.2**.
- **TIP-Position Control** window of the LABVIEW GUI can be used for optimization of the signal
- **NOTE** The minimum second-harmonic power requirement for the Autocorrelator to operate is 1 nanowatt. If the average power of the second harmonic is less than 1 nanowatt, the input pulse energy must be increased and adjusted by slowly rotating the half-wave plate of the beam attenuator.

- Set the *Home* position on the *Measurement* window to the value from the *Position Control* window corresponding to the maximum second harmonic signal.

B. Pulse width measurement and data fitting

An example screenshot of the GUI with an already taken measurement is shown in **Figure T3**.

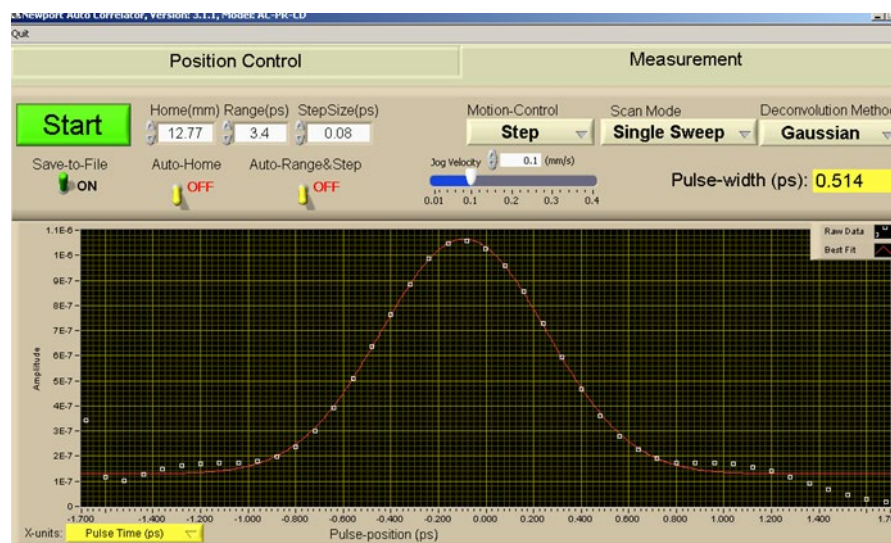


Figure T3 An example of the measured pulse width

In accordance with the description of the method provided in **Section 4.1**, the following procedure is applied for determining the duration (width) of the laser pulses:

- a) the second harmonic signal is registered as a function of the of optical delay distance between two pulses;
- b) the registered data can be represented in time domain by converting the delay distance to time coordinates;
- c) using the computer, the functions are determined (Gaussian, sech^2 , Lorentzian, etc.) which give the best fit to the registered data;
- d) the pulse duration is finally determined by applying the factors corresponding to autocorrelation function (see **Table 4.1**).

Steps **a)** to **d)** are repeated at different positions of pulse-compressor unit (see **Figure T2**) in order to record **the dependence of the measured pulse duration on the prism position**.

NOTE. It is highly recommended to switch-off the HV before changing the position of the compressor prism. Autocorrelator input pulse energy is tuned if necessary, before a measurement at new prism position.

Results are summarized, discussed and reported. Experimental setting and result data are saved and the report form in **APPENDIX B** is filled in.

Task 2. Laser pulse duration effect on energy spread of the accelerated electron bunches

The aim of this Task is to apply laser-operational skills and measurement results obtained upon completion of Task 1 in an experiment on AREAL facility. Specifically, effect of laser pulse duration on beam energy spread will be tried to be observed by varying the pulse duration according **to the dependence on the prism position** already measured in Task 1. The work is performed jointly and in correlation with the group of students involved in the corresponding Experimental Task of the Joint Course (Electron Beam Parameter Measurements).

- Only standard procedures with remote control for the pulse duration described in Task 1 will be required.

Results are presented in a freeform report.

Further Reading

1. Jean-Claude Diels, Wolfgang Rudolph, Ultrashort Laser Pulse Phenomena, 2nd Edition, Academic Press, 2006, **ISBN:** 9780080466408
2. Claude Rullière (ed.), Femtosecond Laser Pulses: Principles and Experiments: 2nd Edition, 2005, **ISBN** 9780387266749
3. R. Trebino, Frequency-resolved optical gating: the measurement of ultrashort laser pulses, Kluwer Academic Publishers, Boston (2002), **ISBN:** 1402070667 (alk. paper), Boston
4. A useful web site by Rick Trebino, <http://frog.gatech.edu/index.html>
5. T. Rao and D. H. Dowell (eds.), An Engineering Guide to Photoinjectors, Createspace Independent Pub, (2013), **ISBN** 1481943227
6. Description of the topics of this Joint Course, as well as supplement materials can be found on the web site www.candle.am

In case there are problems with access to the referenced literature students can contact the course tutor to obtain electronic copies.

APPENDIX A: Relationship among energy parameters

Figure xx illustrates a regular train of optical pulses of different shapes with **repetition rate** $f = 1/T$, where T is the full period.

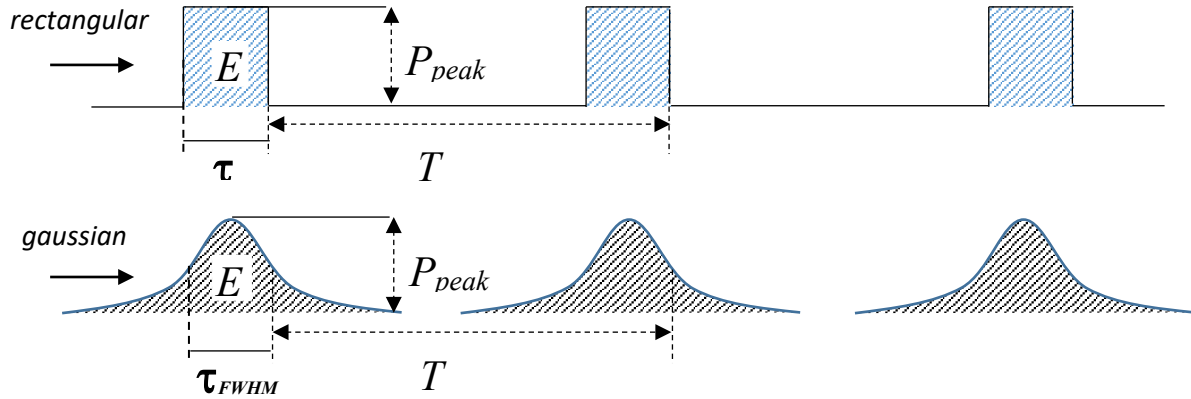


Figure A1. Illustration of pulse several parameters

Let us assume the energy, E , contained in every pulse is constant. Power is the rate of the energy flow or energy per unit time. Depending on the time interval over which the energy flow is considered, two types of power can be defined.

The **peak power**, P_{peak} , is the rate of energy flow in every pulse:

$$P_{peak} = E/\tau,$$

while the **average power**, P_{av} , is the rate of energy flow over one full period:

$$P_{av} = E/T = Ef.$$

The above relationships hold true for rectangular pulses. In the case of other pulse shapes a constant factor has to be included. For instance, the peak power of a Gaussian pulse (see **Figure A1**) is

$$P_{peak} \approx 0.94E/\tau_{FWHM},$$

where τ_{FWHM} is the “full-width-at-half-maximum” (*FWHM*).

Thus, for example, the energy of a laser pulse can be deduced if average power and the repetition rate are known from other measurements.

APPENDIX B: Report Table 1

Experiment settings			
	Value	Units	
Repetition Rate, R		Hz	
Non-attenuated IR pulse energy, E_{tot}		mJ	
Autocorrelator input pulse energy, E_s		uJ	
Pulse compressor position		Number of steps	
Fixed delay stage position		mm	
Results summary			
	Gaussian shape	Sech ² shape	
Pulse duration, ps			
Data file\LabWork\2019\...		
Graphics file\LabWork\2019\...		

